Eur. Phys. J. B **9**, 641–649 (1999)

THE EUROPEAN PHYSICAL JOURNAL B

EDP Sciences

Order by thermal disorder in 2D planar rotator model with dipolar interactions

E. Rastelli[a], A. Carbognani, S. Regina, and A. Tassi

Dipartimento di Fisica dell' Università, and Istituto Nazionale per la Fisica della Materia, Via delle Scienze, 43100 Parma, Italy

Received 4 August 1998

Abstract. The energy of a square planar rotator model of spins interacting *via* dipolar forces is minimized by infinite inequivalent configurations corresponding to spins arranged on four interpenetrating sublattices making angles α, $-\alpha$, $\pi+\alpha$, $\pi-\alpha$ with a reference axis, α being arbitrary. This infinite degeneracy of the ground state is accidental in nature and one expects that it is removed by thermal fluctuations in agreement with Monte Carlo simulation. Indeed we find that the elementary excitation energies which depend on α lead to a free energy which is a function of α with minima at $\alpha = 0$ and $\alpha = \pi/2$ corresponding to columnar configurations. This selection of columnar configurations out of the infinite ground state manifold is an example of *order by thermal disorder*.

PACS. 75.10.Hk Classical spin models – 75.30.Ds Spin waves

1 Introduction

Dipolar interaction is a spin-spin long range coupling that raises interesting theoretical questions [1,2] and becomes crucial to explain the behaviour of magnetic systems with small exchange interaction [3,4]. Minimum energy spin configurations, elementary excitation energy and thermal behaviour of spin systems with long range interaction are interesting theoretical arguments that can be investigated by low temperature expansions and Monte Carlo (MC) simulations. Possible ferromagnetic order supported by dipolar interaction in cubic lattices was studied a long time ago [1]. Several types of *columnar* spin configurations were found to minimize the energy of orthorhombic and tetragonal lattices [5]. More recently the interest was turned to 1D [4] and 2D [6] spin models in order to investigate the effect of dipolar interactions on long range order (LRO) occurring at low temperature, and to explain some experimental data from elastic and inelastic neutron scattering measurements performed on actual systems. Different kinds of anisotropy and exchange couplings have been introduced to fit experimental data on $CsNiF_3$, a hexagonal quasi 1D ferromagnet [4] of the ABX_3 structure, and on $ErBa_2Cu_3O_7$, an orthorhombic quasi 2D antiferromagnet [6] of the $RBa_2Cu_3O_7$ family, where R is a rare earth ion.

Here we focus on the basic properties of the two-component spin model (planar rotator model) on a square (SQ) lattice with dipolar interactions. In particular, we investigate the existence of a low temperature ordered phase. It is well known that LRO is ruled out in a 2D spin model with continuous symmetry when the spin-spin interaction is short ranged [7]. On the other hand, long range interactions may or may not support LRO in the 2D planar model. For instance, spin-spin interactions decaying as $1/r^3$, where r is the spin-spin distance, are believed to support LRO when the interaction is ferromagnetic [8], whereas no LRO is expected when the interaction is antiferromagnetic on the basis of MC simulation [9].

The question is still open when the spins are coupled by dipolar interactions. In this case the ground state spin configuration [10] was looked for assuming a four-sublattice configuration. An infinite degeneracy was obtained since any configuration where the spins along a diagonal of the unit cell are antiparallel has the same energy independent of the angle α that the spins make with the x axis chosen parallel to a row of nearest neighbour (NN) spins. MC simulation [11] suggests this degeneracy to be removed at finite temperature where a columnar spin configuration with rows (columns) of parallel spins pointing along the x (y) axis alternate along the y (x) axis. So far no theoretical support to this expectation has been provided. Here we evaluate the elementary excitation energy of the planar rotator model and we take thermal fluctuations into account to investigate the mechanism selecting a columnar spin configuration. We find that the minimum of the free energy is obtained for columnar spin configurations ($\alpha = 0$ or $\alpha = \pi/2$) in agreement with MC expectations [11]. This selection is caused by the fact that the elementary excitation energy does depend on α: this is an additional example of *order by thermal disorder* [12–14]. Indeed the ground state degeneracy is accidental in nature because it is not related to symmetry properties of the Hamiltonian so that one expects that the infinite degeneracy

[a] e-mail: `rastelli@pr.infn.it`

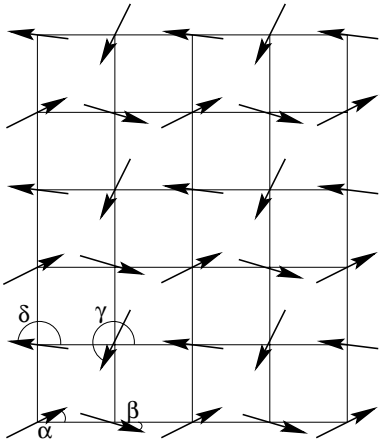

Fig. 1. Four sublattice configuration assumed to minimize the ground state energy.

of the ground state does not survive thermal fluctuations. We find that the selection of columnar configurations is also confirmed by MC simulation on large enough samples.

2 Minimum energy configuration

The Hamiltonian of the planar rotator model of two component spins interacting *via* dipolar interactions reads

$$\mathcal{H} = -\frac{1}{2}\frac{\mu^2}{a^3}\sum_{\substack{i,\mathbf{r}\\ \mathbf{r}\neq 0}}\sum_{\rho\sigma} f^{\rho\sigma}(\mathbf{r}) S_i^\rho S_{i+\mathbf{r}}^\sigma \tag{2.1}$$

where

$$f^{\rho\sigma}(\mathbf{r}) = \frac{a^3}{r^3}\left(3\frac{r^\rho r^\sigma}{r^2} - \delta_{\rho,\sigma}\right). \tag{2.2}$$

In equation (2.1) μ is the magnetic moment; $\rho, \sigma = x, y$ label the two spin components; i labels the N sites of a square (SQ) lattice; $\mathbf{r} = m_1 a\hat{\mathbf{u}}_x + m_2 a\hat{\mathbf{u}}_y$, with m_1, m_2 integers, is the generic lattice vector; a is the lattice constant. In order to investigate the ground state spin configuration we start with a four-sublattice model in agreement with the proposal of reference [10]. The four two-component spins of the unit cell are

$$\mathbf{S}_i^a = S\cos(\alpha + \psi_i^a)\hat{\mathbf{u}}_x + S\sin(\alpha + \psi_i^a)\hat{\mathbf{u}}_y \tag{2.3}$$
$$\mathbf{S}_i^b = S\cos(\beta + \psi_i^b)\hat{\mathbf{u}}_x + S\sin(\beta + \psi_i^b)\hat{\mathbf{u}}_y \tag{2.4}$$
$$\mathbf{S}_i^c = S\cos(\gamma + \psi_i^c)\hat{\mathbf{u}}_x + S\sin(\gamma + \psi_i^c)\hat{\mathbf{u}}_y \tag{2.5}$$
$$\mathbf{S}_i^d = S\cos(\delta + \psi_i^d)\hat{\mathbf{u}}_x + S\sin(\delta + \psi_i^d)\hat{\mathbf{u}}_y. \tag{2.6}$$

As shown in Figure 1 $\alpha, \beta, \gamma, \delta$ are the angles the spins of the unit cell make with the x axis in the ground state and ψ_i^s $(s = a, b, c, d)$ are the angular displacements from the ground state configuration. At low temperature the angular displacements are small and one can expand (2.3-2.6) in powers of them. We introduce this expansion in Hamiltonian (2.1) and retain all terms up to second order in ψ_i^s. Finally we write the angular displacements in terms of their Fourier transforms

$$\psi_i^s = \sqrt{\frac{4}{N}}\sum_{\mathbf{q}} \psi_{\mathbf{q}}^s e^{i\mathbf{q}\cdot\mathbf{r}_i} \tag{2.7}$$

and we obtain the harmonic approximation of Hamiltonian (2.1)

$$\mathcal{H}_2 = E_0 + \frac{1}{2}\frac{\mu^2 S^2}{a^3}\sum_{ss'}\sum_{\mathbf{q}} \psi_{\mathbf{q}}^s A_{\mathbf{q}}^{ss'} \psi_{-\mathbf{q}}^{s'} \tag{2.8}$$

where

$$\begin{aligned} E_0 = -\frac{1}{4}\frac{\mu^2 S^2 N}{a^3}\big\{ & 2D^{xx}(0) + W_{1x}^{xx}(0)(\cos\alpha\cos\beta \\ & + \cos\gamma\cos\delta + \sin\alpha\sin\delta + \sin\beta\sin\gamma) \\ & + W_{1y}^{xx}(0)(\cos\alpha\cos\delta + \cos\beta\cos\gamma + \sin\alpha\sin\beta \\ & + \sin\gamma\sin\delta) + W_2^{xx}(0)(\cos\alpha\cos\gamma + \cos\beta\cos\delta \\ & + \sin\alpha\sin\gamma + \sin\beta\sin\delta)\big\}. \end{aligned} \tag{2.9}$$

The diagonal coefficients $A_{\mathbf{q}}^{ss}$ are given by

$$\begin{aligned} A_{\mathbf{q}}^{aa} = {} & D^{xx}(0) - D^{xx}(\mathbf{q})\sin^2\alpha - D^{yy}(\mathbf{q})\cos^2\alpha \\ & + D^{xy}(\mathbf{q})\sin 2\alpha + W_{1x}^{xx}(0)(\cos\alpha\cos\beta + \sin\alpha\sin\delta) \\ & + W_{1y}^{xx}(0)(\cos\alpha\cos\delta + \sin\alpha\sin\beta) \\ & + W_2^{xx}(0)\cos(\alpha - \gamma), \end{aligned} \tag{2.10}$$

$A_{\mathbf{q}}^{bb}$, $A_{\mathbf{q}}^{cc}$, $A_{\mathbf{q}}^{dd}$ are obtained from $A_{\mathbf{q}}^{aa}$ by the change $\alpha \leftrightarrow \beta$ and $\delta \leftrightarrow \gamma$, $\alpha \leftrightarrow \gamma$ and $\beta \leftrightarrow \delta$, $\alpha \leftrightarrow \delta$ and $\beta \leftrightarrow \gamma$, respectively.

The off-diagonal coefficients $A_{\mathbf{q}}^{ss'} = A_{\mathbf{q}}^{s's}$ are given by

$$\begin{aligned} A_{\mathbf{q}}^{ab} = {} & -W_{1x}^{xx}(\mathbf{q})\sin\alpha\sin\beta \\ & - W_{1x}^{yy}(\mathbf{q})\cos\alpha\cos\beta + W_{1x}^{xy}(\mathbf{q})\sin(\alpha + \beta), \end{aligned} \tag{2.11}$$

$$\begin{aligned} A_{\mathbf{q}}^{ac} = {} & -W_2^{xx}(\mathbf{q})\sin\alpha\sin\gamma \\ & - W_2^{yy}(\mathbf{q})\cos\alpha\cos\gamma + W_2^{xy}(\mathbf{q})\sin(\alpha + \gamma), \end{aligned} \tag{2.12}$$

$$\begin{aligned} A_{\mathbf{q}}^{ad} = {} & -W_{1y}^{xx}(\mathbf{q})\sin\alpha\sin\delta \\ & - W_{1y}^{yy}(\mathbf{q})\cos\alpha\cos\delta + W_{1y}^{xy}(\mathbf{q})\sin(\alpha + \delta), \end{aligned} \tag{2.13}$$

$A_{\mathbf{q}}^{bc}$ is obtained from $A_{\mathbf{q}}^{ad}$ by the change $\alpha \to \beta$ and $\delta \to \gamma$, $A_{\mathbf{q}}^{bd}$ from $A_{\mathbf{q}}^{ac}$ by the change $\alpha \to \beta$ and $\gamma \to \delta$, $A_{\mathbf{q}}^{cd}$ from $A_{\mathbf{q}}^{ab}$ by the change $\alpha \to \gamma$ and $\beta \to \delta$. The dipolar sums

appearing in equations (2.9-2.13) are given by

$$D^{\rho\sigma}(\mathbf{q}) = \sum_{\mathbf{R}\neq 0} f^{\rho\sigma}(\mathbf{R})\cos(\mathbf{q}\cdot\mathbf{R}) \tag{2.14}$$

$$W_{1x}^{\rho\sigma}(\mathbf{q}) = \sum_{\mathbf{R}} f^{\rho\sigma}(\mathbf{R}+a\hat{\mathbf{u}}_x)\cos[\mathbf{q}\cdot(\mathbf{R}+a\hat{\mathbf{u}}_x)] \tag{2.15}$$

$$W_{1y}^{\rho\sigma}(\mathbf{q}) = \sum_{\mathbf{R}} f^{\rho\sigma}(\mathbf{R}+a\hat{\mathbf{u}}_y)\cos[\mathbf{q}\cdot(\mathbf{R}+a\hat{\mathbf{u}}_y)] \tag{2.16}$$

$$W_{2}^{\rho\sigma}(\mathbf{q}) = \sum_{\mathbf{R}} f^{\rho\sigma}(\mathbf{R}+a\hat{\mathbf{u}}_x+a\hat{\mathbf{u}}_y)\cos[\mathbf{q}\cdot(\mathbf{R}+a\hat{\mathbf{u}}_x+a\hat{\mathbf{u}}_y)] \tag{2.17}$$

where $\mathbf{R} = 2m_1 a\hat{\mathbf{u}}_x + 2m_2 a\hat{\mathbf{u}}_y$ is the generic vector of a SQ lattice with a four-spin unit cell. Minimization of E_0 (Eq. (2.9)) with respect to α, β, γ, δ, gives the ground state configuration of the model. We obtain

$$\begin{aligned}\frac{\partial E_0}{\partial\alpha} = -\frac{1}{4}\frac{\mu^2 S^2 N}{a^3}\big[&W_{1x}^{xx}(0)(-\sin\alpha\cos\beta+\cos\alpha\sin\delta)\\ &+W_{1y}^{xx}(0)(-\sin\alpha\cos\delta+\cos\alpha\sin\beta)\\ &+W_{2}^{xx}(0)(-\sin\alpha\cos\gamma+\cos\alpha\sin\gamma)\big]=0.\end{aligned} \tag{2.18}$$

The remaining three minimum equations are obtained in the following way: $\frac{\partial E_0}{\partial\beta}$ is obtained by equation (2.18) by the change $\alpha\leftrightarrow\beta$, and $\gamma\leftrightarrow\delta$; $\frac{\partial E_0}{\partial\gamma}$ is obtained by equation (2.18) by the change $\alpha\leftrightarrow\gamma$, and $\beta\leftrightarrow\delta$; $\frac{\partial E_0}{\partial\delta}$ is obtained by equation (2.18) by the change $\alpha\leftrightarrow\delta$, and $\beta\leftrightarrow\gamma$. The solution is

$$\alpha = \text{arbitrary}, \quad \beta=-\alpha, \quad \gamma=\pi+\alpha, \quad \delta=\pi-\alpha. \tag{2.19}$$

Solution (2.19) leads to the following ground state energy

$$\begin{aligned}E_0 &= -\frac{1}{2}\frac{\mu^2 S^2 N}{a^3}\big[D^{xx}(0)+W_{1x}^{xx}(0)+W_{1y}^{xx}(0)-W_2^{xx}(0)\big]\\ &= -2.5495\frac{\mu^2 S^2 N}{a^3}\end{aligned} \tag{2.20}$$

where the final result is obtained by the numerical evaluation of dipolar sums (2.14-2.17). Note that E_0 is independent of α. This means infinite degeneracy of the ground state. The stability of the above result, based on the assumption of a four-sublattice spin configuration, will be tested in the next section.

3 Elementary excitations and free energy

In order to test the stability of the assumed ground state configuration we evaluate the elementary excitation spectra. To this aim we diagonalize Hamiltonian (2.8) and we obtain

$$\mathcal{H}_2 = E_0 + \frac{1}{2}\frac{\mu^2 S^2}{a^3}\sum_{\ell=1}^{4}\sum_{\mathbf{q}}\lambda_{\mathbf{q}}^{\ell}\phi_{\mathbf{q}}^{\ell}\phi_{-\mathbf{q}}^{\ell} \tag{3.1}$$

where the eigenvalues $\lambda_{\mathbf{q}}^{\ell}$ of Hamiltonian (2.8) are

$$\begin{aligned}\lambda_{\mathbf{q}}^{1,2} = {}& D^{xx}(0)+W_{1x}^{xx}(0)-W_{1y}^{xx}(0)-W_2^{xx}(0)\\ &-\big[D^{yy}(\mathbf{q})+W_2^{yy}(\mathbf{q})\big]\cos^2\alpha\\ &-\big[D^{xx}(\mathbf{q})+W_2^{xx}(\mathbf{q})\big]\sin^2\alpha\\ &\mp\Big\{\big[D^{xy}(\mathbf{q})+W_2^{xy}(\mathbf{q})\big]^2\sin^2(2\alpha)\\ &+\big[(W_{1x}^{xx}(\mathbf{q})+W_{1y}^{xx}(\mathbf{q}))\sin^2\alpha\\ &-(W_{1y}^{yy}(\mathbf{q})+W_{1x}^{yy}(\mathbf{q}))\cos^2\alpha\big]^2\Big\}^{1/2}\end{aligned} \tag{3.2}$$

$$\begin{aligned}\lambda_{\mathbf{q}}^{3,4} = {}& D^{xx}(0)+W_{1x}^{xx}(0)-W_{1y}^{xx}(0)\\ &-W_2^{xx}(0)-\big[D^{yy}(\mathbf{q})-W_2^{yy}(\mathbf{q})\big]\cos^2\alpha\\ &-\big[D^{xx}(\mathbf{q})-W_2^{xx}(\mathbf{q})\big]\sin^2\alpha\\ &\mp\Big\{\big[D^{xy}(\mathbf{q})-W_2^{xy}(\mathbf{q})\big]^2\sin^2(2\alpha)\\ &+\big[(W_{1x}^{xx}(\mathbf{q})-W_{1y}^{xx}(\mathbf{q}))\sin^2\alpha\\ &+(W_{1y}^{yy}(\mathbf{q})-W_{1x}^{yy}(\mathbf{q}))\cos^2\alpha\big]^2\Big\}^{1/2}.\end{aligned} \tag{3.3}$$

As one can see from (3.2-3.3) the elementary excitation spectra $\lambda_{\mathbf{q}}^{\ell}$ are periodic functions of α. Indeed $\lambda_{\mathbf{q}}^{\ell}(\alpha) = \lambda_{\mathbf{q}}^{\ell}(\alpha+\pi)$. Configurations with $\alpha=0$ and $\alpha=\pi/2$ correspond to *columnar* configurations. Indeed the choice $\alpha=0$ ($\alpha=\pi/2$) corresponds to alternating rows (columns) of parallel spins pointing along the x (y) axis. The elementary excitation spectra for selected directions in the reciprocal space are given in Figures 2 and 3 for $\alpha=0$ and $\alpha=\pi/4$, respectively.

As one can see the eigenvalues $\lambda_{\mathbf{q}}^{\ell}$ are well defined for any $\mathbf{q}$ so that the four sublattice spin configuration we have assumed to describe the ground state is stable against spontaneous fluctuations. The spectra for $\alpha=\pi/2$ are the same as for $\alpha=0$ provided that $(1,0)$ and $(0,1)$ directions are exchanged. At $\mathbf{q}=0$ one has $D^{xx}(0)=D^{yy}(0)=0.5642$, $W_{1x}^{xx}(0)=W_{1y}^{yy}(0)=4.2429$, $W_2^{xx}(0)=W_2^{yy}(0)=1.0320$, $W_{1y}^{xx}(0)=W_{1x}^{yy}(0)=-1.3237$, $D^{xy}(0)=W_2^{xy}(0)=0$, and the elementary excitations (3.2-3.3) are

$$\begin{aligned}&\lambda_{\mathbf{q}=0}^{1,2} = 3.5026 \mp 2.9192|\cos(2\alpha)|,\\ &\lambda_{\mathbf{q}=0}^{3}=0, \quad \lambda_{\mathbf{q}=0}^{4}=11.1332.\end{aligned} \tag{3.4}$$

Note that $\lambda_{\mathbf{q}=0}^{3}=0$ for any α. This soft mode corresponds to fluctuations driving a columnar spin configuration into a generic configuration of the infinitely degenerate manifold.

The relationship between $\psi_{\mathbf{q}}^{s}$ defined in equation (2.7) and $\phi_{\mathbf{q}}^{\ell}$ appearing in equation (3.1) is given by

$$\psi_{\mathbf{q}}^{s} = \sum_{\ell=1}^{4} u_s^{\ell}\phi_{\mathbf{q}}^{\ell} \tag{3.5}$$

where u_s^{ℓ} are the eigenvectors belonging to the eigenvalues $\lambda_{\mathbf{q}}^{\ell}$ given in equations (3.2-3.3).

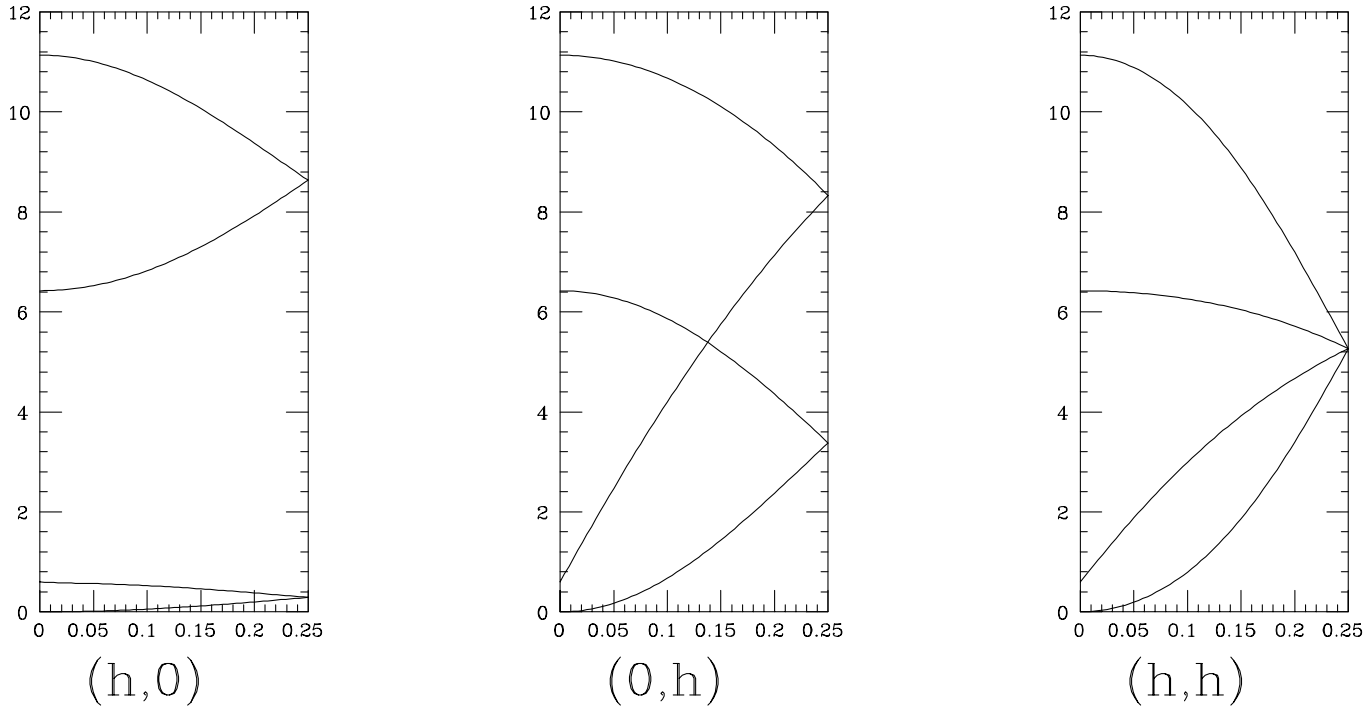

Fig. 2. Elementary excitation energies along (1, 0), (0, 1), (1, 1) directions of the reciprocal lattice for $\alpha = 0$.

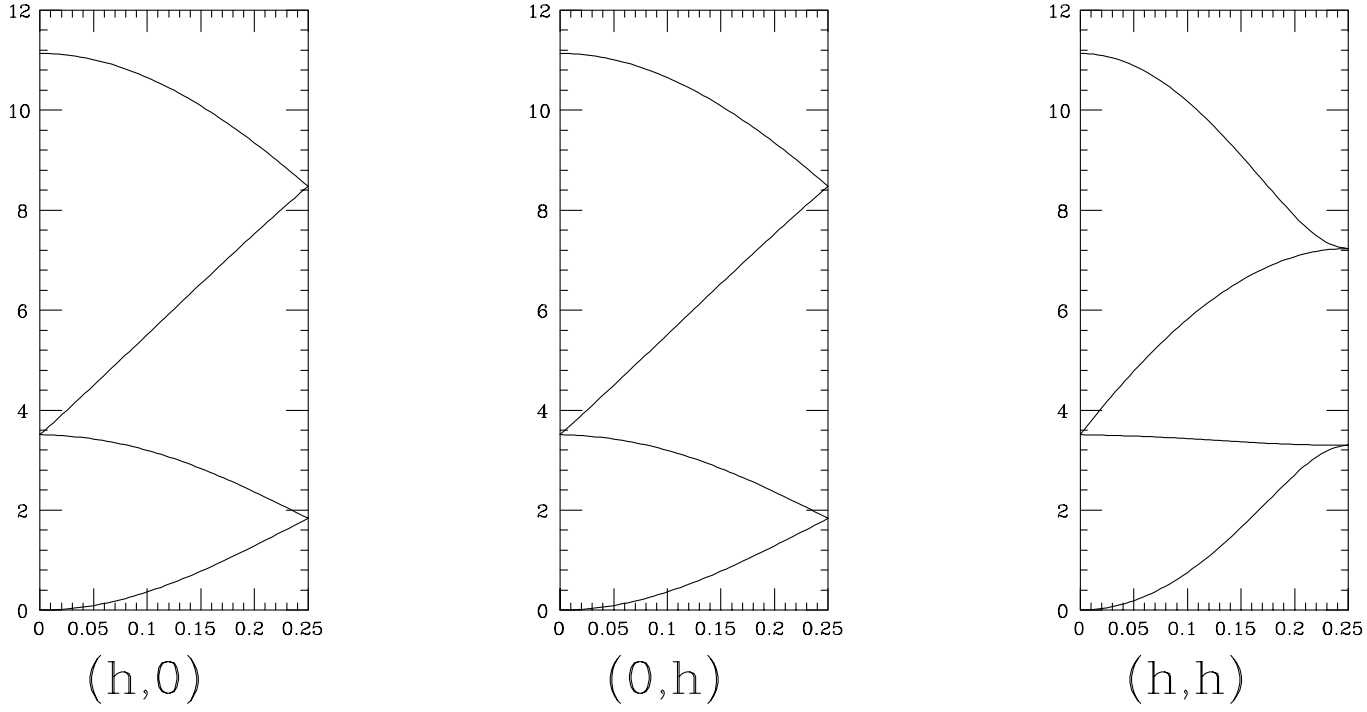

Fig. 3. Elementary excitation energies along (1, 0), (0, 1), (1, 1) directions of the reciprocal lattice for $\alpha = \pi/4$.

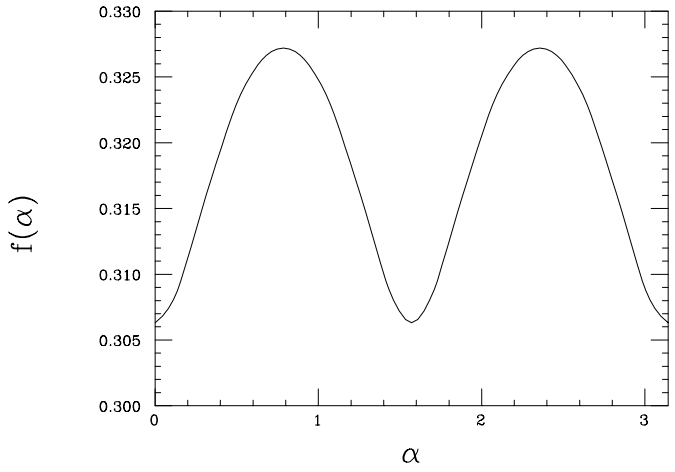

Fig. 4. The thermal fluctuations contritution to the free energy as function of the angle characterizing the infinite degeneracy of the ground state. See equation (3.8).

The Helmholtz free energy in harmonic approximation is

$$\mathcal{F} = E_0 - k_{\rm B}T \ln \int \mathcal{D}\phi \exp\Big\{ - \frac{\mu^2 S^2}{2k_{\rm B}Ta^3} \sum_{\ell=1}^{4} \sum_{\mathbf{q}} \lambda_{\mathbf{q}}^{\ell} |\phi_{\mathbf{q}}^{\ell}|^2 \Big\}$$
$$= E_0 - \frac{1}{2} k_{\rm B}TN \ln \Big(\frac{k_{\rm B}Ta^3}{2\pi\mu^2 S^2} \Big) + \frac{1}{2} k_{\rm B}TN f(\alpha) \tag{3.6}$$

where

$$f(\alpha) = \frac{1}{N} \sum_{\mathbf{q}} \sum_{\ell=1}^{4} \ln \lambda_{\mathbf{q}}^{\ell}. \tag{3.7}$$

Equation (3.7) gives the α dependent contribution to the free energy coming from thermal fluctuations. In Figure 4 we show the numerical evaluation of $f(\alpha)$ as function of α. Note that $f(\alpha) = f(\alpha + \pi/2)$ as expected on the basis of the symmetry properties of the eigenvalues $\lambda_{\mathbf{q}}^{\ell}$. As one can see the minima of $f(\alpha)$ occur at $\alpha = 0$, $\alpha = \pi/2$ so that thermal fluctuations select columnar states out of the manifold of the infinite degeneracy. Order is supported by thermal disorder.

4 Monte Carlo simulation

In this section we present Monte Carlo (MC) simulation using an approach which is an extension of the approach introduced by reference [15] This approach is suitable to take into account dipolar interactions because it avoids truncation of the long range tail of the interaction. It is based on a periodic arrangement of MC cells and it has been worked out for Ising models [15,16]. We generalize this method in order to investigate the planar rotator model. We write the Hamiltonian (2.1) in the following way

$$\mathcal{H} = -\frac{1}{2}\mu^2 \frac{N}{L^2} \sum_{\rho\sigma} \Bigg[\sum_{\mathbf{n}} \sum_{\mathbf{G}\neq 0} f^{\rho\sigma}(\mathbf{G}) S_{\mathbf{n}}^{\rho} S_{\mathbf{n}+\mathbf{G}}^{\sigma}$$
$$+ \sum_{\substack{\mathbf{n},\mathbf{n}' \\ \mathbf{n}\neq\mathbf{n}'}} \sum_{\mathbf{G}} f^{\rho\sigma}(\mathbf{n}-\mathbf{n}'+\mathbf{G}) S_{\mathbf{n}}^{\rho} S_{\mathbf{n}'+\mathbf{G}}^{\sigma} \Bigg] \tag{4.1}$$

where $\mathbf{n}$, $\mathbf{n}'$ label the sites of a square cell containing $L \times L$ spins; $\mathbf{G} = m_1 La\hat{\mathbf{u}}_x + m_2 La\hat{\mathbf{u}}_y$ is a vector joining the spin at site $\mathbf{n}$ with the spin at site $\mathbf{n}+\mathbf{G}$. We assume a periodic arrangement of the cells that means $\mathbf{S}_{\mathbf{n}+\mathbf{G}} = \mathbf{S}_{\mathbf{n}}$ according to reference [15]. Hamiltonian (4.1) becomes

$$\mathcal{H} = -\frac{1}{2}\mu^2 S^2 \frac{N}{L^2} \Bigg\{ V_0 L^2$$
$$+ \sum_{\substack{\mathbf{n},\mathbf{n}' \\ \mathbf{n}\neq\mathbf{n}'}} \big[V^{xx}(\mathbf{n}-\mathbf{n}') \cos\theta_{\mathbf{n}} \cos\theta_{\mathbf{n}'}$$
$$+ V^{yy}(\mathbf{n}-\mathbf{n}') \sin\theta_{\mathbf{n}} \sin\theta_{\mathbf{n}'}$$
$$+ V^{xy}(\mathbf{n}-\mathbf{n}') \sin(\theta_{\mathbf{n}} + \theta_{\mathbf{n}'}) \big] \Bigg\} \tag{4.2}$$

where

$$\sum_{\mathbf{G}\neq 0} f^{\rho\sigma}(\mathbf{G}) = V_0 \delta_{\rho\sigma} \tag{4.3}$$

$$\sum_{\mathbf{G}} f^{\rho\sigma}(\mathbf{n}-\mathbf{n}'+\mathbf{G}) = V^{\rho\sigma}(\mathbf{n}-\mathbf{n}') = V^{\rho\sigma}(\mathbf{n}'-\mathbf{n}) \tag{4.4}$$

and $\theta_{\mathbf{n}}$ is the angle the spin at site $\mathbf{n}$ makes with x axis. In evaluating the sum over cells in (4.3) and (4.4) we find that the convergence of the sums is obtained accounting for at least 10^4 cells. In any case we have evaluated the sum for 4×10^6 cells. The quantities $V^{\rho\sigma}(\mathbf{n}-\mathbf{n}')$ were calculated for each couple $\mathbf{n}-\mathbf{n}' = n_x\hat{\mathbf{u}}_x + n_y\hat{\mathbf{u}}_y$ before starting MC simulation. Since n_x and n_y can be positive as well as negative we took advantage of the following identities coming from the symmetry of the square lattice:

$$\begin{aligned} V^{xx}(n_x,n_y) &= V^{xx}(-n_x,n_y) = V^{xx}(n_x,-n_y) \\ &= V^{xx}(-n_x,-n_y) \\ V^{yy}(n_x,n_y) &= V^{xx}(n_y,n_x) \\ V^{xy}(n_x,n_y) &= V^{xy}(-n_x,-n_y) = -V^{xy}(-n_x,n_y) \\ &= -V^{xy}(n_x,-n_y) \\ V^{xy}(n_x,n_y) &= V^{xy}(n_y,n_x). \end{aligned} \tag{4.5}$$

In order to perform MC simulation we move a spin at site $\mathbf{n}_0$ leaving all the remaining spins unchanged and we evaluate the energy cost comparing the energy of the system after and before the move. The energy involved in a random change of the angle of the generic spin $\mathbf{S}_{\mathbf{n}_0}$ from $\theta_{\mathbf{n}_0}$

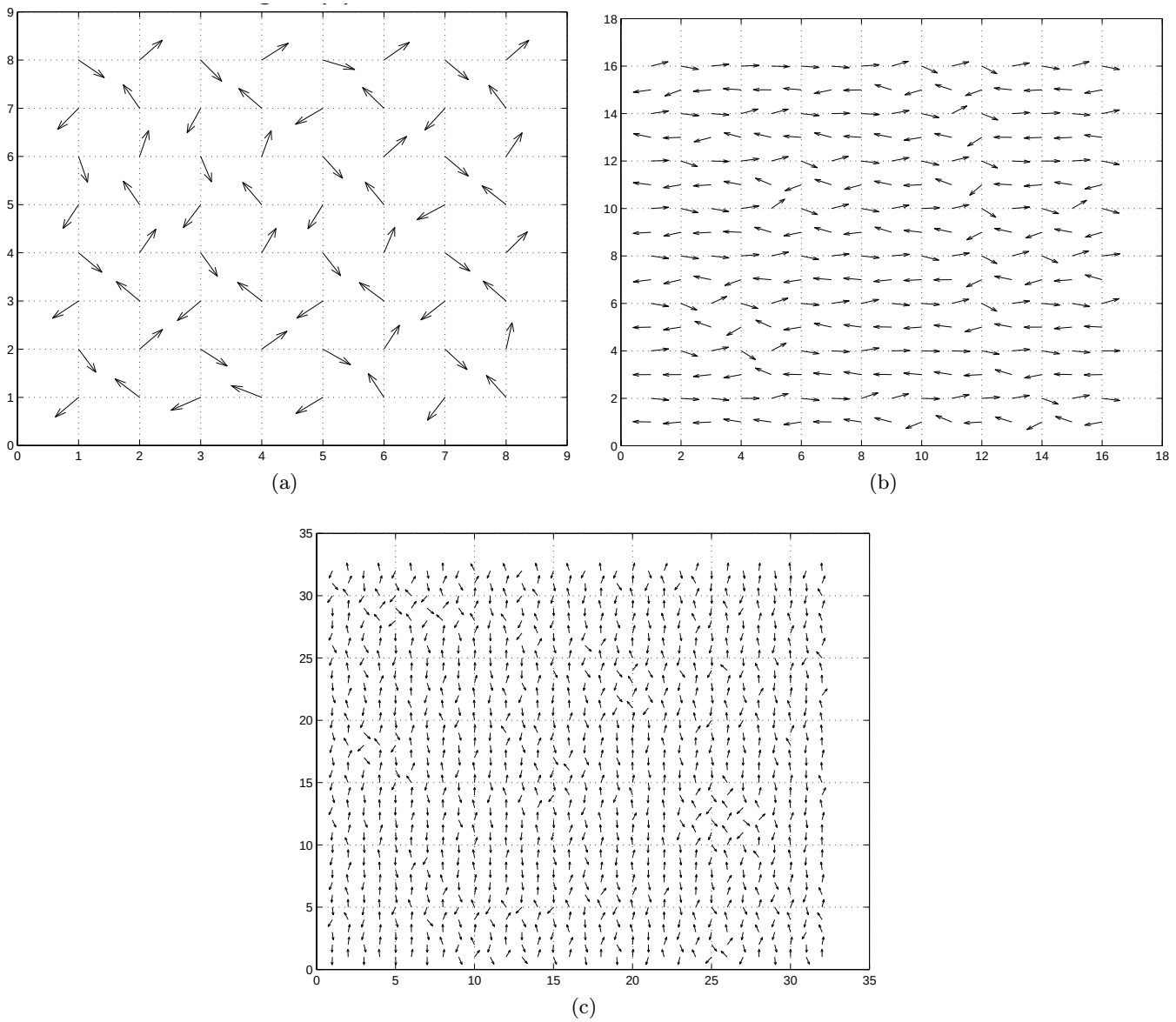

Fig. 5. Snapshot of 8×8 (a), 16×16 (b), 32×32 (c) samples at $T = 0.1$.

to $\theta'_{\mathbf{n}_0}$ is

$$\begin{aligned}\Delta E = -\mu^2 S^2 \Big\{ & (\cos\theta'_{\mathbf{n}_0} - \cos\theta_{\mathbf{n}_0}) \\ & \times \sum_{\mathbf{n}\neq\mathbf{n}_0} \left[V^{xx}(\mathbf{n}-\mathbf{n}_0)\cos\theta_{\mathbf{n}} + V^{xy}(\mathbf{n}-\mathbf{n}_0)\sin\theta_{\mathbf{n}} \right] \\ & + (\sin\theta'_{\mathbf{n}_0} - \sin\theta_{\mathbf{n}_0}) \\ & \times \sum_{\mathbf{n}\neq\mathbf{n}_0} \left[V^{yy}(\mathbf{n}-\mathbf{n}_0)\sin\theta_{\mathbf{n}} + V^{xy}(\mathbf{n}-\mathbf{n}_0)\cos\theta_{\mathbf{n}} \right] \Big\}. \end{aligned} \tag{4.6}$$

MC simulation were performed using the traditional Metropolis procedure: the thermal probability of a spin move $p = \exp(-\Delta E/k_{\mathrm{B}}T)$ is compared with a random number z chosen between 0 and 1. The spin move is then accepted if and only if $z < p$. Simulations were carried out on square lattices of size $L = 4$ to $L = 32$ starting from a random configuration and performing 10^5 equilibration MC steps. A MC step is defined, as usual, as sequentially stepping through the lattice moving each spin once. Because of the long range nature of the interaction the typical computing time required for a single MC step is much longer than the time required for systems with nearest neighbour exchange interaction. The time required to perform 10^5 MC steps goes from 5 seconds for a $L = 4$ lattice up to 5 hours for a $L = 32$ lattice using a Silicon Graphics Onix Infinite Reality2 machine.

We have pushed our MC simulation towards lower temperatures with respect to previous simulations [11] in order to get snapshots of the spin configurations with less and less thermal noise. For small lattices ($L = 4, 8$)

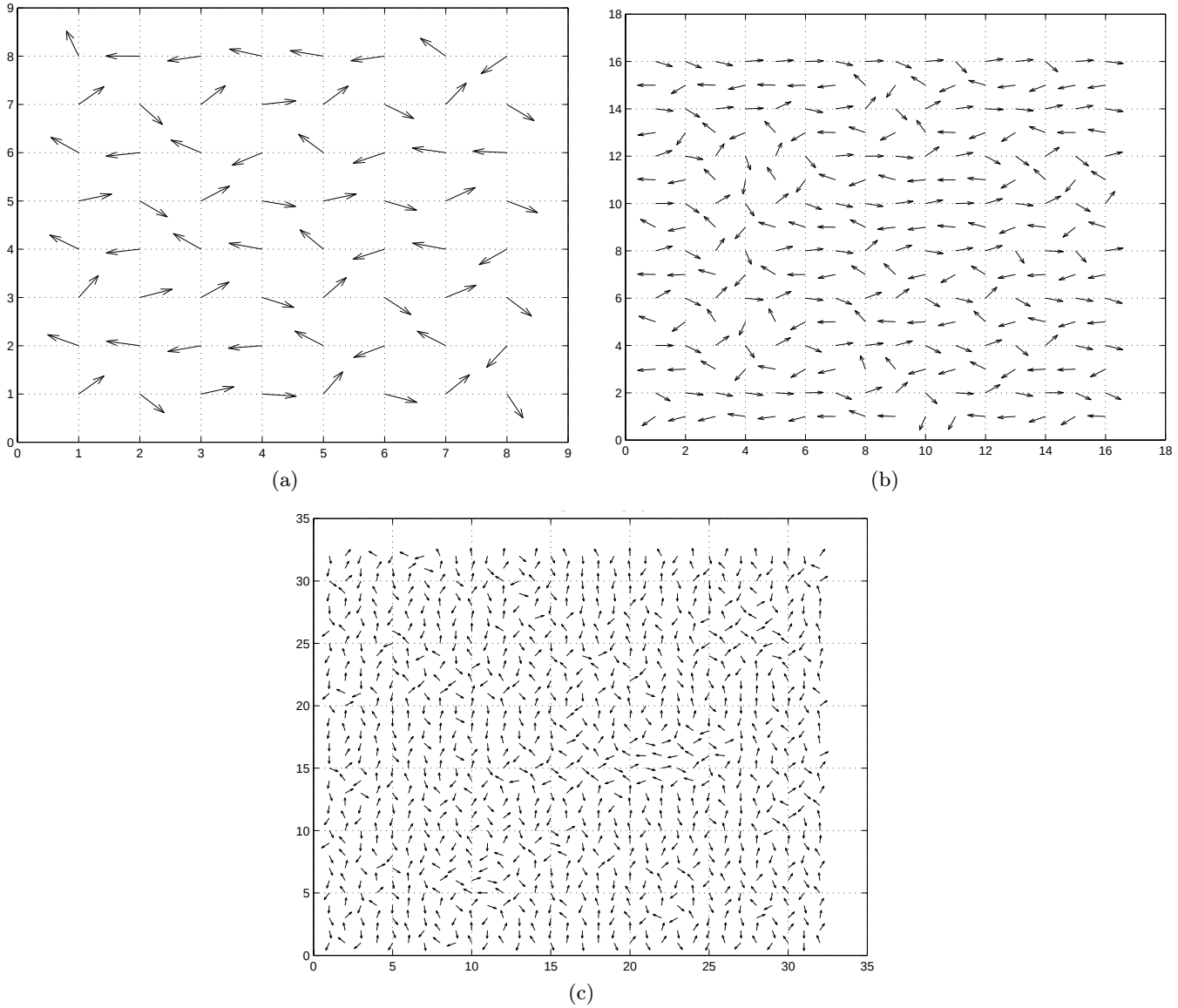

Fig. 6. Snapshot of 8×8 (a), 16×16 (b), 32×32 (c) samples at $T = 0.4$.

the results are strongly dependent on the initial random configuration and on the number of thermalization steps. This is because the spins experience all the states of the infinitely degenerate manifold. As L increases ($L = 16, 32$) the state selected by MC simulation is the same as expected by analytic calculation ($\alpha = 0$ or $\alpha = \pm 90°$). Figures 5 show snapshots of samples with $L = 8, 16, 32$, respectively, at $T \equiv k_{\rm B}Ta^3/\mu^2S^2 = 0.1$. Note that finite size effects are evident in cases a) and b), where the infinite degeneracy of the ground state affects the average angles that the spins of the unit cell make with the x axis. In case a) the average angles are $\alpha = -131.7°$, $\beta = 129.5°$, $\gamma = 180° - 122.7°$, $\delta = 180° + 130°$. In case b) they are $\alpha = 171.4°$, $\beta = -171.5°$, $\gamma = 180° + 170.1°$, $\delta = 180° - 170.9°$. In case c) the results are independent of the starting random configuration and of the number of thermalization steps. The average angles are $\alpha = -90.5°$, $\beta = 90.3°$, $\gamma = 180° - 90.8°$, $\delta = 180° + 90.8°$. The selection of $\alpha \simeq -90°$ agrees with the analytic result. A similar behaviour is observed at $T = 0.4$ as shown in Figures 6. Note that many domain-like defects occur as temperature is increased.

We have evaluated by MC simulation specific heat

$$C = \frac{\langle \mathcal{H}^2 \rangle - \langle \mathcal{H} \rangle^2}{N k_{\rm B} T^2} \tag{4.7}$$

and staggered susceptibility

$$\chi_{\rm st} = \frac{1}{N} \left[\langle \mathbf{S}_{\rm st}^2 \rangle - \langle \mathbf{S}_{\rm st} \rangle^2 \right] \tag{4.8}$$

where $\mathbf{S}_{\rm st} = \sum_i \mathrm{e}^{i\mathbf{Q}\cdot\mathbf{r}_i} \mathbf{S}_i$ is the staggered magnetization and $\mathbf{Q}$ is the wave vector characterizing the order of the columnar phase. Specific heat and staggered susceptibility

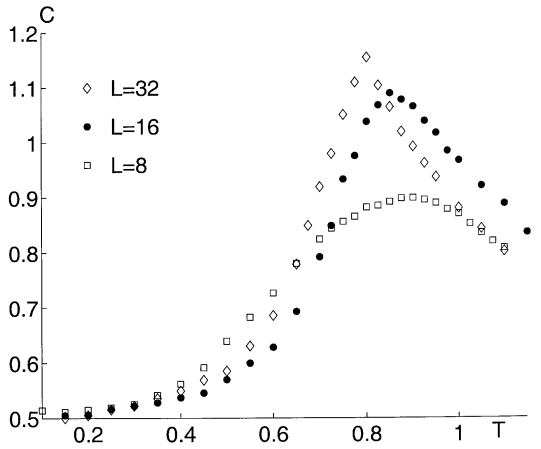

Fig. 7. Specific heat as function of temperature for different lattice sizes: $L = 8$ (open squares), $L = 16$ (full circles), $L = 32$ (diamonds).

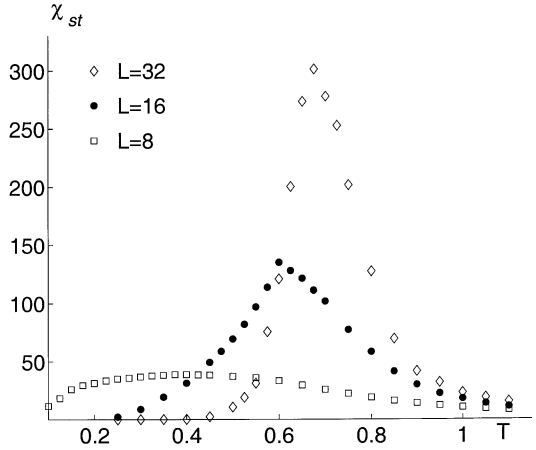

Fig. 8. Staggered susceptibility as function of temperature for different lattice sizes: $L = 8$ (open squares), $L = 16$ (full circles), $L = 32$ (diamonds).

are evaluated for lattices with $L = 4, 8, 12, 16, 24, 32$. All calculations start from an ordered columnar spin configuration at $T = 0.1$. The system is then heated up to $T = 1.2$ by steps of $\Delta T = 0.025$. In Figures 7 and 8 we show the specific heat and the staggered susceptibility, respectively, obtained by MC simulation for lattices with $L = 8, 16, 32$. As expected, the temperature of the maximum of specific heat and staggered susceptibility is size dependent. In particular, the temperature at which the maximum of specific heat occurs decreases as L increases. On the contrary the temperature of the maximum of the staggered susceptibility increases as L increases. As shown in Figure 9 the size-dependent temperatures of the maxima converge toward $T = 0.75$ in the thermodynamic limit, so that this value may be assumed as the critical temperature of the SQ planar model with dipolar interactions. This value is in agreement with that obtained by MC evaluation of the specific heat for a lattice with $L = 40$ [11]. Note that the critical temperature of the planar model is much lower than the critical temperature of the corresponding Ising model with dipolar interactions $T = 1.95$ [16].

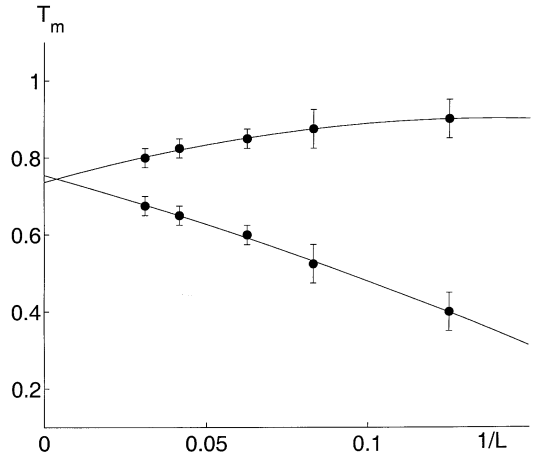

Fig. 9. Critical temperature as obtained by the maximum of the specific heat (higher curve) and of the staggered susceptibility (lower curve) as function of the lattice size.

5 Summary and conclusions

The ground state of the SQ planar rotator model with spins interacting *via* dipolar forces is characterized by infinite isoenergetic configurations consisting of four sublattice spin patterns [10]. The angle the spins of each sublattice make with the x axis is α, -α, $\pi + \alpha$, $\pi - \alpha$, with α arbitrary. On the other hand MC simulations [11] support the occurrence of columnar spin configurations corresponding to $\alpha = 0$ or $\alpha = \pi/2$. In order to test whether this expectation is correct we have evaluated the elementary excitation energies which are found to depend on α as shown in Figures 2 and 3. This fact implies that the free energy is in its turn a function of α with minima at $\alpha = 0$ and $\alpha = \pi/2$ as shown in Figure 4. Note that the selection of one state occurs at finite temperature so that this model gives one more example of *order by thermal disorder*. In addition our results may test the nature of the spin-spin interactions in compounds like $RBa_2Cu_3O_7$ (where R is a rare earth). The spin ordering observed in those compounds have been ascribed to dipolar interactions [3,5]. MC simulation has been performed on a SQ Ising model with dipolar interactions in order to investigate thermal behaviour of $ErBa_2Cu_3O_7$ [16]. The critical temperature of the model was found to be $T_{\rm I} = 1.95 \frac{(g_y \mu_{\rm B} S)^2}{k_{\rm B} a^3}$. Inelastic neutron scattering data [17] and crystal electric field (CEF) approximation allow the evaluation of the anisotropic effective g-factor leading to $g_x = 7.42$, $g_y = 8.04$, $g_z = 4.57$ [6]. Substitution of g_y in the critical temperature obtained by MC simulation on the Ising model gives $T_{\rm I} = 0.38$ K, somewhat below the observed critical temperature $T_{\rm c} = 0.62$ K [3,18]. It is clear that the Ising model is a raw description of the localized spins in $ErBa_2Cu_3O_7$ because the y axis is certainly the easy axis but CEF calculation leads to non vanishing values of g_x and g_z. A more realistic treatment based on the planar model, for which $g_x = g_y$, $g_z = 0$ provides a critical

temperature $T_{\rm P} = 0.75\frac{(g_y\mu_{\rm B}S)^2}{k_{\rm B}a^3}$ leading to $T_{\rm P} = 0.13$ K assuming $g_x \simeq g_y = 8.04$. The critical temperature obtained from the planar model is even worse than the corresponding one obtained from the Ising model. Moreover, we expect that taking g_z into account, an even lower critical temperature should be obtained because of the out-of-plane fluctuations, so that other kinds of interactions such as exchange coupling and anisotropy have to be called for.

In conclusion we stress that the SQ planar model with dipolar interaction exhibits interesting properties but thermal behaviour of compounds like $ErBa_2Cu_3O_7$ can be explained only by accounting for anisotropies and exchange interactions [6] as well as dipolar interactions.

This research was supported in part by Consiglio Nazionale delle Ricerche. The authors would thank Dr. S. Allodi for computational support and Centro di Calcolo Elettronico dell'Università di Parma for the access to Silicon Graphics Onix Infinite Reality2 parallel machine.

References

1. M.H. Cohen, F. Keffer, Phys. Rev. **99**, 1135 (1955).
2. C. Pich, F. Schwabl, Phys. Rev. B **47**, 7957 (1993).
3. T.W. Clinton, J.W. Lynn, J.Z. Liu, Y.X. Jia, T.J. Goodwill, R.N. Shelton, B.W. Lee, M. Buchgeister, M.B. Maple, J.L. Peng, Phys. Rev. B **51**, 5429 (1995).
4. M. Baehr, M. Winkelmann, P. Vorderwisch, M. Steiner, C. Pich, F. Schwabl, Phys. Rev. B **54**, 12932 (1996).
5. S.K. Misra, J. Felsteiner, Phys. Rev. B **46**, 11033 (1992).
6. E. Rastelli, A. Tassi, Eur. Phys. J. B **4**, 285 (1998).
7. N.D. Mermin, H. Wagner, Phys. Rev. Lett. **17**, 1133 (1966).
8. M.E. Fisher, S. Ma, B.G. Nickel, Phys. Rev. Lett. **29**, 917 (1972).
9. S. Romano, Phys. Rev. B **44**, 7066 (1991).
10. P.I. Belobrov, R.S. Gekht, V.A. Ignatchenko, Sov. Phys. JETP **57**, 636 (1983).
11. S. Romano, Nuovo Cim. **9**, 409 (1987).
12. J. Villain, R. Bideaux, J.P. Carton, R. Conte, J. Phys. France **41**, 1263 (1980).
13. C.L. Hanley, Phys. Rev. Lett. **62**, 2056 (1989)
14. E. Rastelli, S. Sedazzari, A. Tassi, J. Phys.-Cond. Matter **3**, 5861 (1991).
15. R. Kretschmer, K. Binder, Z. Phys. B **34**, 375 (1979).
16. A.B. MacIsaac, J.P. Whitehead, K. De'Bell, K. Sowmya Narayanan, Phys. Rev. B **46**, 6387 (1992).
17. J. Mesot, P. Allenspach, U. Staub, A. Furrer, H. Mutka, R. Osborn, A. Taylor, Phys. Rev. B **47**, 6027 (1993).
18. Y. Nakazawa, M. Ishikawa, T. Takabatake, Physica B **148**, 404 (1987).